Environmental Science
Water Research & Technology

PAPER

View Article Online
View Journal | View Issue

Cite this: *Environ. Sci.: Water Res. Technol.*, 2024, **10**, 551

Industrial waste against pollution: mill scale-based magnetic hydrogels for rapid abatement of Cr(VI)†

Autchariya Boontanom,*[a] Marina Maddaloni,[bc] Piyada Suwanpinij,[f] Irene Vassalini *[bde] and Ivano Alessandri *[bde]

This work studies the adsorption of hexavalent chromium from water using magnetic composite hydrogels obtained by combining magnetite micropowders, synthesized from industrial by-products, with a natural biopolymer (alginate) and other active species that could be obtained from food waste, like ascorbic acid. In particular, mill scale was collected from a steel hot strip mill, converted into magnetite microparticles and encapsulated in alginate-based hydrogel bubbles, in combination with activated carbon (AC) and L-ascorbic acid (VitC). The synergistic combination of each active component creates an efficient, multifunctional hybrid adsorbing unit, which enables the total abatement of Cr(VI) from contaminated water, even at a high concentration range (up to 50 mg L^{-1}). Alginate plays the double role of water-absorbing and Cr(VI)-adsorbing matrix as well as that of carrier and container for the other active components, among which AC is utilized as an extra-adsorbing unit for Cr(VI), while VitC enables reduction of Cr(VI). Furthermore, the presence of Fe_3O_4 microparticles endows the hydrogel bubbles with magnetic responsiveness, enabling their easy removal at the end of their decontaminant activity by means of small magnets. The adsorption capability of the Fe_3O_4/AC/VitC-alginate hydrogels was tested under different conditions: Cr^{6+} was completely abated within 60 minutes when the Cr(VI) concentration in ultrapure water was equal to 20 mg L^{-1}, and within 360 minutes when the concentration in ultrapure water was 50 mg L^{-1}, without need of any pH-regulating treatment. The role of each different active unit was investigated and compared to the adsorption performances of whole composite systems, elucidating cooperative effects and deriving optimized formulations. The composite hydrogels were also tested in real contaminated water in the presence of other possible common competitive inorganic species and in non-acidic pH. Under these conditions it was also possible to obtain complete Cr(VI) removal, even if with slower kinetics, and 93% Cr(VI) (50 mg L^{-1}) was abated within 60 minutes.

Received 5th July 2023,
Accepted 3rd January 2024

DOI: 10.1039/d3ew00490b

rsc.li/es-water

Water impact

Here we demonstrate that magnetite particles recovered from mill scale can be associated with ascorbic acid and incorporated into water-absorbing alginate hydrogel bubbles that can be used for water remediation. The synergistic combination of components with specific functions (highly adsorbent gels, redox-active molecules, magnetic particles) allows Cr(VI) to be efficiently adsorbed-even at the very high concentration of 50 mg L^{-1} and reduced to Cr(III). After use, the bubbles can be easily collected with small magnets, enabling full recovery of Cr(III) and its reuse.

1. Introduction

The steel industry generates several by-products that can have a deep impact on the environment and should be recovered and properly recycled.[1,2] For example, over 13.5 million tons of mill scale, an iron-rich by-product that is generated in casting, soaking, reheating and rolling processes, are annually generated worldwide.[3] Unfortunately, usually it is underexploited and simply disposed of in landfills.[4]

In parallel, chromic acid (H_2CrO_4) is a strong and corrosive oxidising agent widely used as a concentrated solution in metal finishing industries such as electroplating, dyeing, and ceramic glazing.[5] In the past years, there has been a growing concern

[a] *The Sirindhorn International Thai-German Graduate School of Engineering (TGGS), King Mongkut's University of Technology North Bangkok, 10800 Bangkok, Thailand*
[b] *INSTM, UdR Brescia, Italy*
[c] *Chemistry for Technologies Laboratory, Mechanical and Industrial Engineering Department (DIMI), University of Brescia, Via Branze 38, 25123 Brescia, Italy*
[d] *Department of Information Engineering (DII), University of Brescia, Via Branze 38, 25123 Brescia, Italy. E-mail: ivano.alessandri_at_unibs.it*
[e] *INO-CNR, Via Branze 38, 25123 Brescia, Italy*
[f] *Metallurgy and Metal Forming, Leibniz-Institut für Werkstofforientierte Technologien (IWT), Badgasteiner Straße 3, 28359 Bremen, Germany*
† Electronic supplementary information (ESI) available. See DOI: https://doi.org/10.1039/d3ew00490b

about the use of chromic acid and its derivatives. In fact, hexavalent chromium is a highly toxic and carcinogenic pollutant, and human exposure to it can cause irritations in the respiratory system even at a very low dosage. Moreover, Cr(VI) is soluble but not biodegradable in water.[6] Therefore, a proper method for Cr(VI) removal must be considered carefully before discarding wastewater into sewages.

Among several approaches such as chemical precipitation,[7] electrocoagulation,[8,9] and filtration,[10,11] adsorption is known for its simplicity, low production cost, and wide selection of materials.[12] The uptake of Cr(VI) can occur by physisorption, chemisorption, and bioremediation through either conventional or non-conventional adsorbents.[13] Examples of popular conventional adsorbents are commercial activated carbon, inorganic materials (*i.e.* zeolite and silica gel), and various types of ion exchange resins.[14,15] Although these adsorbents are known for their abundance and efficiency against Cr(VI), there still are major drawbacks, such as high costs, which limit their usage in larger-scale applications, and difficulty in recovery or maintenance of the adsorbents themselves.[16,17] Moreover, the demand for green and sustainable wastewater remediation has been increasing globally: the new-generation adsorbents should not only provide fast adsorption but also meet some ecological and economic criteria, such as a production process characterized by low cost and low environmental impact and biocompatibility.[18,19]

Therefore, compound adsorbents such as metal organic frameworks (MOFs)[20–22] and composite hydrogels[23,24] have recently emerged as versatile materials for many fields of applications, including adsorption of dissolved matter in aqueous solutions. In particular, hydrogels obtained from natural polymers and modified with magnetic nanoparticles were proved to be efficient and sustainable allies in environmental remediation, by combining the non-toxicity, biocompatibility and biodegradability properties of the polymeric network with the ease of recovery *via* a magnetic field.[25,26]

In this work we selected alginate as a natural biopolymer. It can be extracted from algae and is commercially available. Alginate has been widely used for the preparation of hydrogels by calcium cross-linking.[27] As an anionic polymer, alginate is conventionally utilized for fabricating hydrogels that are conventionally used for adsorption of positively charged pollutants, like Pb(II), Cu(II), As(III) and As(V).[28–31] Nevertheless, due to the presence in its chemical structure of several hydroxyl and carboxylic groups that are able to bind with multivalent heavy metal ions, many recent studies have demonstrated its adsorptive behaviour also against negatively charged heavy metals like Cr(VI).[32,33] In particular, with reference to Cr(VI)-containing pollutants as the anionic CrO_4^{2-} (chromate) and $Cr_2O_7^{2-}$ (dichromate) species, examples of efficient removal are reported in the literature by using either composite Fe_3O_4@Alg–Ce bubbles or nano zero-valent iron/carbon/alginate systems.[34–36] However, in both these cases, the magnetic responsiveness was obtained through commercial magnetic nanoparticles, which contributed to increasing the cost of the adsorbent as a whole.[37] This magnetic function is fundamental for assisting facile separation of the adsorbent system from wastewater, but it should be replaced by cheaper alternatives, such as magnetic microparticles obtained from iron sand or mill scale.[38–40] In this way, beyond the economic advantage, it is possible to achieve a key benefit from the environmental point of view, since industrial wastes and by-products have a high impact in several applications of technology.

This work aimed at synthesizing an efficient and environment-friendly hydrogel system for Cr(VI) removal endowed with magnetic responsiveness provided by Fe_3O_4 microparticles obtained from mill scale. To pursue this scope and maximize the interaction with Cr(VI), alginate was combined with other chemical components: activated carbon (AC) and ascorbic acid (VitC). The high efficiency of the composite hydrogel was confirmed by adsorption tests in water contaminated with Cr(VI) (20 and 50 mg L^{-1}) in the presence or in the absence of competing species. Within this system, all the building blocks cooperate and carry out complementary functions: activated carbon and the alginate matrix adsorb Cr(VI) ions, vitamin C reduces Cr(VI) to Cr(III)[41,42] and chelates Cr(III) to prevent any possible secondary pollution,[43] while Fe_3O_4 confers magnetic responsiveness to the whole system.

Even if all the chemical properties and functionalities of the single components are well known, to the best of our knowledge, it is the first time that they have been combined to create a very effective system for Cr(VI) removal. In addition, as anticipated, magnetite microparticles used for the preparation of the hydrogel were produced starting from an industrial waste (ferrous oxide scale derived from a hot strip rolling mill), further increasing the environmental sustainability and circularity of the proposed system.

2. Materials and methods

2.1. Synthesis and characterization of Fe_3O_4 powder

Ferrous oxide scale derived from a hot strip rolling mill, which is a black flaky by-product of the iron rolling process collected from the drained water, was ground and sieved to the size of 75–180 μm. It was then converted into Fe_3O_4 using a combination of calcination and hydrogen reduction processes.[36] The industrial waste was firstly calcined at 800 °C for 120 min to ensure the formation of a homogeneous Fe_2O_3 phase and eliminate impurities. It was subsequently reduced by calcination at 650 °C for 240 min in the presence of a reducing atmosphere (mixed gas H_2 + Ar + H_2O).[44,45]

The resulting black powder was characterized by X-ray diffraction (Aeris, Malvern PanAnalytical, using a Cu anode), Raman spectroscopy (Labram HR-800, Horiba Jobin-Yvon, using a He–Ne laser source (λ = 632.8 nm)), and field-emission scanning electron microscopy (Regulus FE-SEM8230, Hitachi, magnification × 5.0–10.0k). As regards XRD analysis, the obtained powder was ground in a mortar

and then put in a low-background sample holder for data collection. The XRD pattern was recorded with a scan rate of 0.0108° s^{-1} in the 20°–80° 2θ range. As regards the Raman characterization, the Fe_3O_4 powder was analysed using a 50× microscope objective and a 10% attenuating power filter and setting the acquisition time equal to 10 s.

2.2. Synthesis of alginate-based hydrogel bubbles

With the exception of Fe_3O_4 microparticles, all the other chemical reagents used for the preparation of the composite hydrogels were commercial (they were purchased from Sigma Aldrich): sodium alginate (halal food grade), granular activated carbon Darco® KB-G (size 100 mesh, impurities per 100 g: <0.50% water soluble, <12% moisture, and <200 mg L^{-1} acid soluble iron), L-ascorbic acid (reagent grade, >98%), calcium chloride dihydrate (reagent grade, ≥99.0%) and ethanol (absolute, ≥99.8). All the reactants were dissolved in ultrapure Milli-Q water obtained from Integral 5 water purification system.

After an optimization process of the synthesis protocol (see ESI S1†), to prepare the composite hydrogel bubbles, 0.1 g of mill scale-derived Fe_3O_4, 0.07 g activated carbon, and 0.1 g L-ascorbic acid were added into a solution of 0.2 g sodium alginate and 5 mL Milli-Q water. The solution was then sonicated for 15 minutes to ensure the homogeneity. Then, it was added dropwise by means of a syringe to a cross-linking solution containing Ca^{2+}. The cross-linker solution was prepared by using a 0.6 M solution of calcium chloride dihydrate in 100 mL of a mixture of 80 : 20 (V/V) ultrapure Milli-Q water and ethanol. The cross-linking step lasted overnight to create stable hydrogel bubbles. The dimension of the syringe needle as well as of the applied pressure to the syringe piston determined the final bubble dimension, which was in the order of a few millimetres. Generally, for 1 ml of alginate solution about 60 ± 2 bubbles were prepared.

The optimization of the synthesis was performed to maximize bubble stability, homogeneity, and magnetic response, and it is reported in ESI S1.†

Additionally, four reference alginate-based hydrogel bubbles were prepared in a similar way using 0.2 g sodium alginate in 5 mL Milli-Q water as hydrogel matrix material and adding only some of the other components of the previously reported composite system. These alginate-based bubbles include only alginate, alginate + Fe_3O_4, alginate + Fe_3O_4 + AC, and alginate + Fe_3O_4 + VitC. The amount of the reactants used for their preparation is summarized in Table 1.

Table 1 Composition of alginate-based bubbles used as adsorbents and reference materials

Name	Sodium alginate	Fe_3O_4	AC	VitC
Alg	200 mg	—	—	—
Fe_3O_4-alg		100 mg		
Fe_3O_4/AC-alg			70 mg	
Fe_3O_4/VitC-alg			—	100 mg
Fe_3O_4/AC/VitC-alg			70 mg	

2.3. Characterization of hydrogel bubbles

The synthesized hydrogel bubbles were characterized in terms of magnetic response, using an in-house vibrating sample magnetometer (VSM), after evaporating and grinding into dry powder 10 wet bubbles. The characterisation was carried out at room temperature with an operating magnetic field ranging from −10 000 to 10 000 Oe. The obtained data were compared with the magnetic properties of a similar amount of Fe_3O_4 powder (~0.06 g).

The magnetic responsiveness of the hydrated bubbles dispersed in aqueous solutions at room temperature was tested by introducing contact with a common magnet, as illustrated in Video S6† and Fig. 2d.

The composite hydrogel bubbles were subjected also to Raman μ-spectroscopy (Labram HR-800, Horiba Jobin-Yvon, using a He–Ne laser source (λ = 632.8 nm)). One hydrated Fe_3O_4/AC/VitC-alginate bubble was analysed using a 10× microscope objective and a 10% attenuating power filter and setting the acquisition time equal to 20 s.

Fe_3O_4/AC/VitC-alginate bubbles were characterized by Fourier transform infrared spectroscopy (FTIR) using a Nicolet iN10 MX spectrometer operating in attenuated total reflectance (ATR) mode. Also, their thermal stability from room temperature to 800 °C under a nitrogen atmosphere was assessed by means of thermogravimetric analysis (TGA, Mettler Toledo TGA/DSC 3+) at a constant heating rate of 5 °C per minute.

2.4. Preparation of wastewater samples

Four different wastewater samples were prepared using ultrapure Milli-Q water (2 samples) and commercial mineral water (2 samples) (chemical analysis reported in ESI S2†).

For the preparation of wastewater, potassium dichromate purchased from Sigma Aldrich (RPE ACS, 470337) was used. Initially, a stock solution with a very high Cr concentration (2500 mg L^{-1}) was prepared by dissolving 0.706 g of potassium dichromate in 100 mL of Milli-Q water and then diluting with Milli-Q water to obtain wastewater with a Cr concentration equal to 50 mg L^{-1} (medium concentration, MCr) or 20 mg L^{-1} (low concentration, LCr). An analogous procedure was followed for the preparation of real samples using mineral water as diluting solvent (chemical composition reported in ESI S2†). In this case, the obtained solutions were called TtL-MCr (actual medium concentration, Cr = 50 mg L^{-1}) and TtL-LCr (actual low concentration, Cr = 20 mg L^{-1}).

The pH values of all the wastewater batches were measured by means of a pH meter and no pH modification was carried out during adsorption experiments.

The 20 mg L^{-1} Cr(VI) solution prepared in ultrapure water was characterised by a pH of 6.34, the 50 mg L^{-1} Cr(VI) solution prepared in ultrapure water was characterised by a pH of 5.5, the 20 mg L^{-1} Cr(VI) solution prepared in mineral water was characterised by a pH of 7.9, and the 50 mg L^{-1} Cr(VI) solution prepared in mineral water was characterised by a pH of 7.7.

2.5. Adsorption tests

A series of adsorption experiments was carried out to determine the adsorption capability of Fe_3O_4/AC/VitC alginate bubbles at different Cr^{6+} concentrations. All the adsorption experiments were repeated three times.

First of all, the ideal dosage of adsorbent material was investigated by evaluating the variation of Cr(VI) concentration (in percentage) in the solution after contact with a variable number of bubbles. The amount of Cr(VI) solution to be treated was maintained fixed and equal to 5 mL, while four different bubble dosages were investigated: 5 bubbles per mL of Cr(VI) solution, 10 bubbles per mL, 20 bubbles per mL and 30 bubbles per mL. This type of study was made in relation to both Cr(VI) concentrations using solution prepared with ultrapure water. Solution sampling was performed at fixed intervals (1, 5, 15, 30, 60, 90, and 360 min) in order to evaluate the variation of Cr(VI) concentration as a function of time by means of UV-vis spectroscopy.

For all the following experiments, the best performing adsorbent ratio was selected and a total of 100 hydrogel bubbles (average weight of 0.132 ± 0.012 g) was added to 5 mL of the wastewater solutions. In order to study their adsorption capability and obtain the related kinetic adsorption model, they were kept in contact with the Cr(VI) solution for 360–420 min. Solution sampling was performed at fixed intervals (1, 5, 10, 15, 30, 60, 90, 150, 210, 300, 360 and 420 min) in order to evaluate the variation of Cr(VI) concentration as a function of time.

The Cr^{6+} concentration of the starting wastewater and its variation were determined by UV-vis spectrophotometry (Ocean Optics QE65000) by measuring the intensity at the maximum absorption edge (λ = 350–374 nm).[46] The starting MCr and TtL-MCr wastewater samples were diluted 1 : 2 before spectrophotometric analysis.

After the adsorption test, in the case of colourless samples when the Cr^{6+} concentration was lower than the detection limit of direct UV-vis measurement, an indirect measurement of Cr(VI) was performed using diphenylcarbazide (DPC) as complexing agent and marker (US EPA method 7196A).

Briefly, 20 μL of a DPC 0.02 M solution in acetone and 4 μL of 10% (V/V) H_2SO_4 solution were added to each colourless sample of wastewater (976 μL). The mixture was well mixed using a vortex shaker for 5 min. In the presence of Cr^{6+}, the mixture turned from colourless to purple. This colour change was due to the reduction of Cr^{6+} to Cr^{3+} by DPC, resulting in a complex $[CrDPCO]^+$ which can be detected by UV-vis spectrophotometry with an absorbance edge at 540 nm.[46] 1,5 diphenylcarbazide (ACS reagent grade, residue on ignition ≤0.05%) and sulfuric acid (≤97.0%) were purchased from Sigma Aldrich. Fig. S3† shows the absorption spectra related to both direct and indirect detection methods; other details on UV-vis spectrophotometric detection of Cr(VI) can be found in ESI S3.† Direct spectroscopic Cr^{6+} quantification was possible in the concentration range of 1–20 mg L^{-1}, while indirect measurement with DPC was possible in the concentration range of 0.8–0.025 mg L^{-1}.

In correspondence to all the samplings, the adsorption capacity of the bubbles (q_t, mg g^{-1}) was calculated using eqn (1) (Vijayakumar *et al.*, 2012).[47]

$$q_t = (C_0 - C_t) \times (V/m) \quad (1)$$

where C_0 = starting Cr^{6+} concentration (mg L^{-1}), C_t = Cr^{6+} concentration at a particular sampling time (mg L^{-1}), V = volume of Cr^{6+} wastewater solution (L), and m = weight of dried adsorbent bubbles (g).

In the case of wastewater prepared using ultrapure Milli-Q water, when t is equal to 360 min, it was possible to calculate the equilibrium adsorption capacity (q_e, mg g^{-1}). In order to individuate the best kinetic model for the fitting of the adsorption data, the obtained values of q_t and q_e were used for the creation of the graphs corresponding to the different kinetic models, as reported in Fig. S4.†

The adsorption capacity of the Fe_3O_4/AC/VitC alginate bubbles in ultrapure water was compared to those of the other synthesized alginate-based adsorbents, limiting the adsorption time to 60 min. Afterwards, the hydrogel bubbles were separated from the solution using a magnetic stirrer bar encapsulated in PTFE, and the adsorbed Cr(VI) quantity was determined by UV-vis spectroscopy, similarly to that previously reported in the long-time adsorption test.

The adsorption capability of the Fe_3O_4/AC/VitC alginate bubbles was compared also to the activity of activated carbon in the form of free powder. A titration curve was built in order to individuate the amount of Cr(VI) that saturates the adsorption site of AC: increasing amounts of AC (final AC amount in solution: 5 mg, 10 mg, 22.5 mg, 50 mg, 70 mg and 100 mg) were gradually added to 5 ml of Cr(VI) wastewater. The amount of Cr(VI) remaining in solution after each addition was evaluated by UV-vis spectroscopy after the elimination of AC powder by means of centrifugation. This experiment was conducted for both Cr(VI) solutions in ultrapure water.

For comparison, the Cr(VI) removal capability of mill scale-derived Fe_3O_4 microparticles in the form of free powder was investigated: 100 mg of the powder were put in contact with 5 mL of Cr(VI) 20 mg L^{-1} solution and UV-vis spectroscopy was used to calculate the percentage of Cr(VI) removed after 60 min of contact.

Long-time adsorption tests (up to 420 minutes) of the Fe_3O_4/AC/VitC alginate bubbles were conducted following the previously described procedure in the case of Cr(VI) solutions prepared with mineral water (real samples).

3. Results and discussion

This study aimed at combining an industrial waste (ferrous oxide scale derived from a hot strip rolling mill, which was converted into Fe_3O_4 microparticles through a calcination process) with common components (activated carbon,

alginate, and vitamin C), in view of developing a circular, eco-friendly hydrogel system, which can effectively adsorb Cr^{6+} from wastewater with the additional benefit of easy recovery. For this purpose, we prepared a composite system, named Fe_3O_4/AC/VitC-alginate bubbles, in which all the single components were essential for the working of the final system: Fe_3O_4 was necessary to confer magnetic recoverability, alginate enabled a favourable interaction with water solution, passive adsorption and conferred compactness to the composite, AC was used to enhance adsorption properties, while vitamin C was added to combine adsorption with some reducing capabilities in order to convert Cr(VI) into the less problematic Cr(III). A general scheme of the experimental outline is shown in Fig. 1.

The first step was the conversion of the industrial ferrous waste into micrometric Fe_3O_4 powder *via* a series of thermal treatments (see section 2.1 for details). The complete chemical conversion and purity of the obtained products were verified by means of X-ray diffraction and Raman spectroscopy. As can be seen in Fig. 2a, the obtained black powder resulted to be pure Fe_3O_4: all the XRD peaks typical of magnetite, matching well with the characteristic inverse cubic spinel structure (peaks at 2θ = 30° due to the (200) plane, at 36° due to the (311) plane, at 43° due to the (400) plane, at 53° due to the (422) plane, at 57° due to the (511) plane and at 63° due to the (440) plane) were visible, showing a purity of ~99%. Further confirmation of the chemical nature of the synthesized powder was achieved from Raman analysis (Fig. 2b), since the recorded spectrum was characterized by the presence of the main peak at 675 cm^{-1} (due to the A_{1g} mode) and the less intense peaks at 325 cm^{-1} (E_g mode) and 550 cm^{-1} (T_{2g} mode).[48] The absence of any chemical impurity was confirmed also by energy dispersive X-ray (EDX) analysis performed in combination with scanning electron microscopy characterization, which showed that the powder was characterized by a granular morphology (size 75–180 microns) and that the only chemical elements present were iron and oxygen (Fig. S5†). The powder was characterized also in terms of magnetic properties, which were measured by VSM at room temperature (Fig. 2c). Despite being converted from an industrial waste, the saturation magnetisation (M_s) of Fe_3O_4 powder was as high as 75.74 emu g^{-1}, the remnant magnetisation (M_r) was 6.35 emu g^{-1}, and the coercive field (H_c) value was 105.2 Oe (8.37 kA m^{-1}, 0.0105 T). These data suggest that the bulk Fe_3O_4 derived from mill scale exhibited ferromagnetic behaviour.[49] Interestingly, a similar magnetic behaviour was maintained after the immobilization of the F_3O_4 powder inside the alginate matrix, enabling the possibility of driving hydrogel composite bubbles around the space thanks to a common magnet (Fig. 2d and Video S6†). In the case of hydrogel bubbles the M_s and M_r values decreased to 17.43 and 2.10 emu g^{-1}, while the H_c value increased to 140.5 Oe (11.18 kA m^{-1}, 0.014 T). These facts were a consequence of the non-magnetic properties of the alginate matrix;[50] however, these values are still comparable to those usually reported in the literature for magnetic nanoparticles.[51] This fact is possible thanks to the large size of the here-prepared Fe_3O_4 micropowder, which increased the saturation magnetisation of the magnetic materials.[52]

Thus, embedding magnetic microparticles recycled from mill scale waste in alginate matrix allowed the production of magnetically responsive hydrogel bubbles with preferrable characteristic properties such as high M_s, low M_r, and small H_c at room temperature. These properties are promising for application in water purification,[53] since they enable the possibility of fast adsorbent removal after the end of decontamination experiments and its regeneration after magnetic separation.[54] This is a great advantage in comparison to similar alginate-based hydrogel systems previously studied

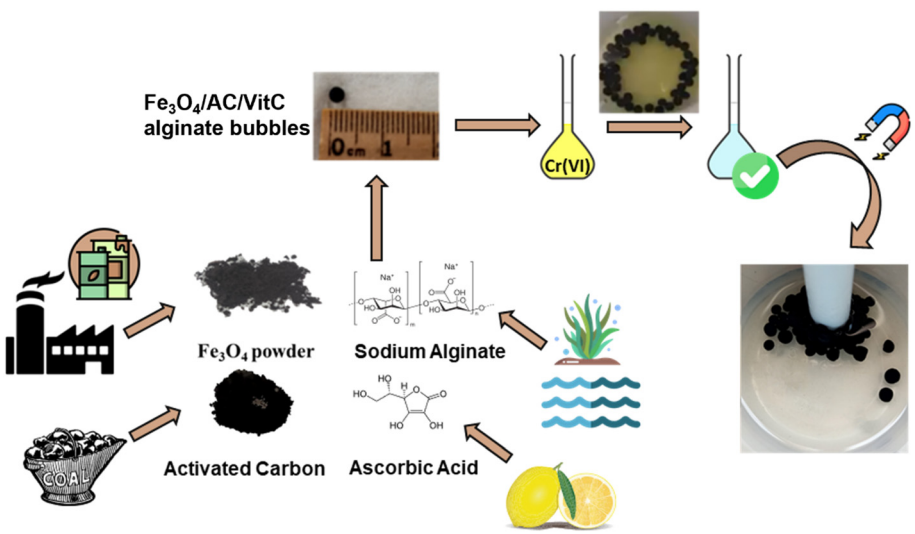

Fig. 1 Experimental outline for the removal of Cr(VI) in wastewater using Fe_3O_4/AC/VitC alginate bubbles. Magnetic Fe_3O_4 micropowder was obtained from mill scale waste and combined with activated carbon, ascorbic acid and alginate in order to obtain hydrogel bubbles, which can be suspended in contaminated water. After Cr(VI) adsorption, the bubbles can be easily removed from the wastewater using a magnetic bar.

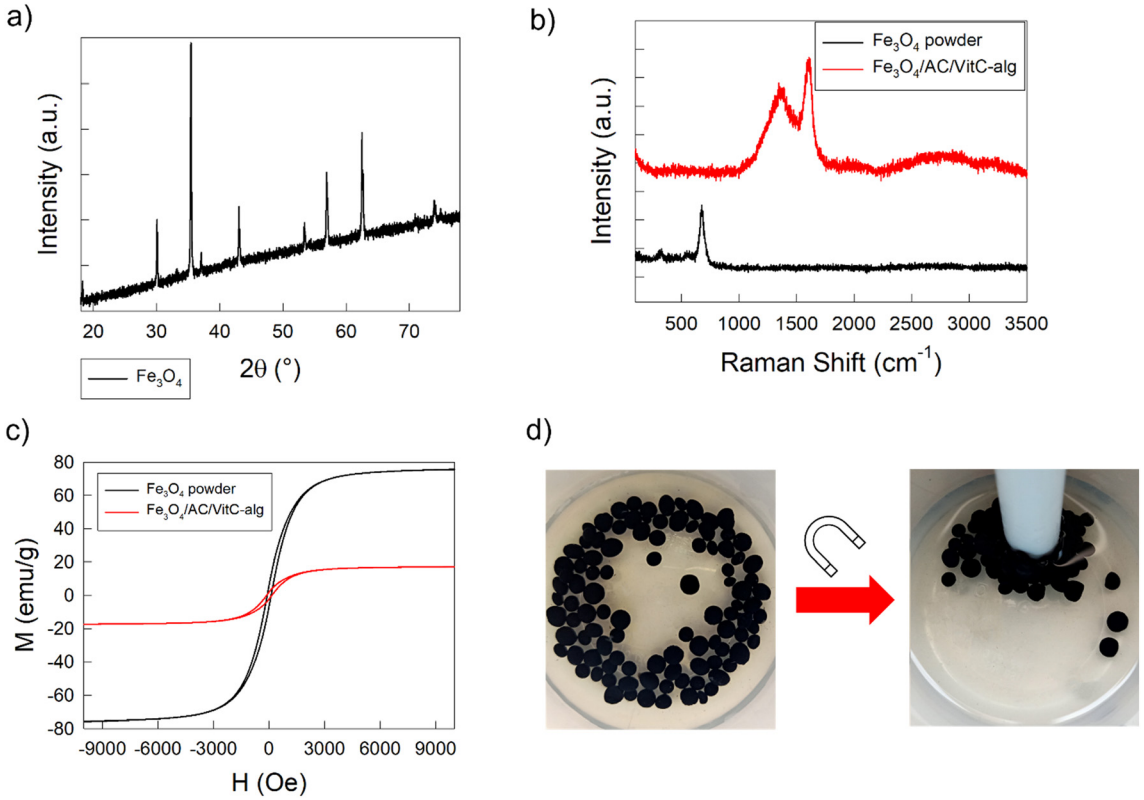

Fig. 2 (a) X-ray diffraction pattern of the Fe_3O_4 powder derived from mill scale. (b) Comparison between the Raman spectra of the Fe_3O_4 powder and the Fe_3O_4/AC/VitC-alg bubbles. (c) Magnetisation curve of Fe_3O_4/AC/VitC hydrogel bubbles in comparison to Fe_3O_4 powder. (d) Pictures showing the magnetic attraction between composite Fe_3O_4/AC/VitC-alg hydrogel bubbles and a common magnet.

by our group for the detection and removal of dyes, pharmaceuticals, and polychlorinated biphenyl compounds.[23,24] In those cases, hydrogel manipulation, motion and removal were possible only by means of filtration or use of tweezers, thanks to bubble stability and millimetric size. However, the possibility of reducing the bubble size and maximizing the surface/mass ratio, which is generally fundamental to maximize the interaction between adsorbents and adsorbates, was precluded.

The size of the prepared hydrogels depends mainly on synthetic parameters, in particular the pressure applied to the syringe piston, dripping rate and diameter (lumen) of the syringe needle. In the present work, we prepared bubbles with a dimension of 2.9 ± 0.6 mm, but in principle, their size could be easily modified according to the requirements.

Their stability at ambient conditions is very high: they can be synthesized in advance and stored in closed containers with water for very long periods (up to six months) without the occurrence of self-degradation or material leaching.

Thermogravimetric analysis performed on dried bubbles (TGA and DTG curves reported in S7†) showed that the first significant weight loss occurred in the temperature range 51–103 °C due to complete dehydration of the bubbles (weight loss ~14%), followed by a second loss step of ~16% of the original weight in the temperature range 230–280 °C (due to thermal degradation of ascorbic acid and alginate, with the fracture of glycosidic bonds, breaking of the alginate backbone and loss of the abundant hydroxyl groups in the form of water) and a more gradual weight loss of a further 15% in the extended temperature range 300–650 °C (due to alginate decarboxylation and release of CO_2).[55–57] In the temperature range 674–712 °C there is another rapid loss of weight (~6%), which usually is not present in TGA curves of alginate-based hydrogels, and is probably due to the release of gaseous molecules from the other components of the composite bubbles (mainly organic gaseous species previously adsorbed on activated carbon). The % of weight remaining at the temperature above 800 °C is ~40%, which is in good agreement with the amount of carbonaceous solid charcoal and inorganic magnetite microparticles introduced into the bubbles during the synthesis.

The synthesized composite bubbles were also characterized by Raman spectroscopy. The Raman spectrum obtained from the Fe_3O_4/AC/VitC-alginate composite bubbles is reported in Fig. 2b, and it is dominated by spectral features of activated carbon, which are characterized by a Raman cross section significantly higher than that of alginate, magnetite, and ascorbic acid. In fact, the Raman spectrum of the composite bubbles showed only two peaks typical of carbonaceous species: the D band, centred at 1360 cm^{-1}, due to lattice defects, disordered arrangement and low symmetry carbon structure, and the G band, centred at 1605 cm^{-1},

which is related to the stretching vibration E_{2g} mode of sp^2 carbon atoms forming the graphite skeleton.[58,59]

They were analysed also by means of ATR-FTIR spectroscopy, as reported in Fig. S8.† The recorded spectrum is characterized by the main peaks of alginate (the spectrum of bubbles made of alginate only is reported as a reference): the peaks centred at 1597 and 1410 cm^{-1} are due to asymmetric and symmetric stretching of C–O–O of carboxylate, while the broad band at ~3300 cm^{-1} is caused by –OH vibrations.[59]

The adsorption efficiency of the composite Fe_3O_4/AC/VitC-alginate bubbles was first investigated against Cr(VI) solutions prepared in ultrapure water at two different concentrations, 20 mg L^{-1} (LCr) and 50 mg L^{-1} (MCr). No pH modification was performed, avoiding the addition of any buffers or chemicals: the operation was maintained as simple as possible to limit the action from external operators and promote the environmental sustainability of the whole decontamination process.

Initially, the optimal adsorbent loading was investigated in order to maximize the adsorption efficiency and rate, maintaining as low as possible the amount of adsorbents. To pursue this scope we tested four different adsorbent loadings: 5 Fe_3O_4/AC/VitC-alginate bubbles per mL of Cr(VI) solution, 10

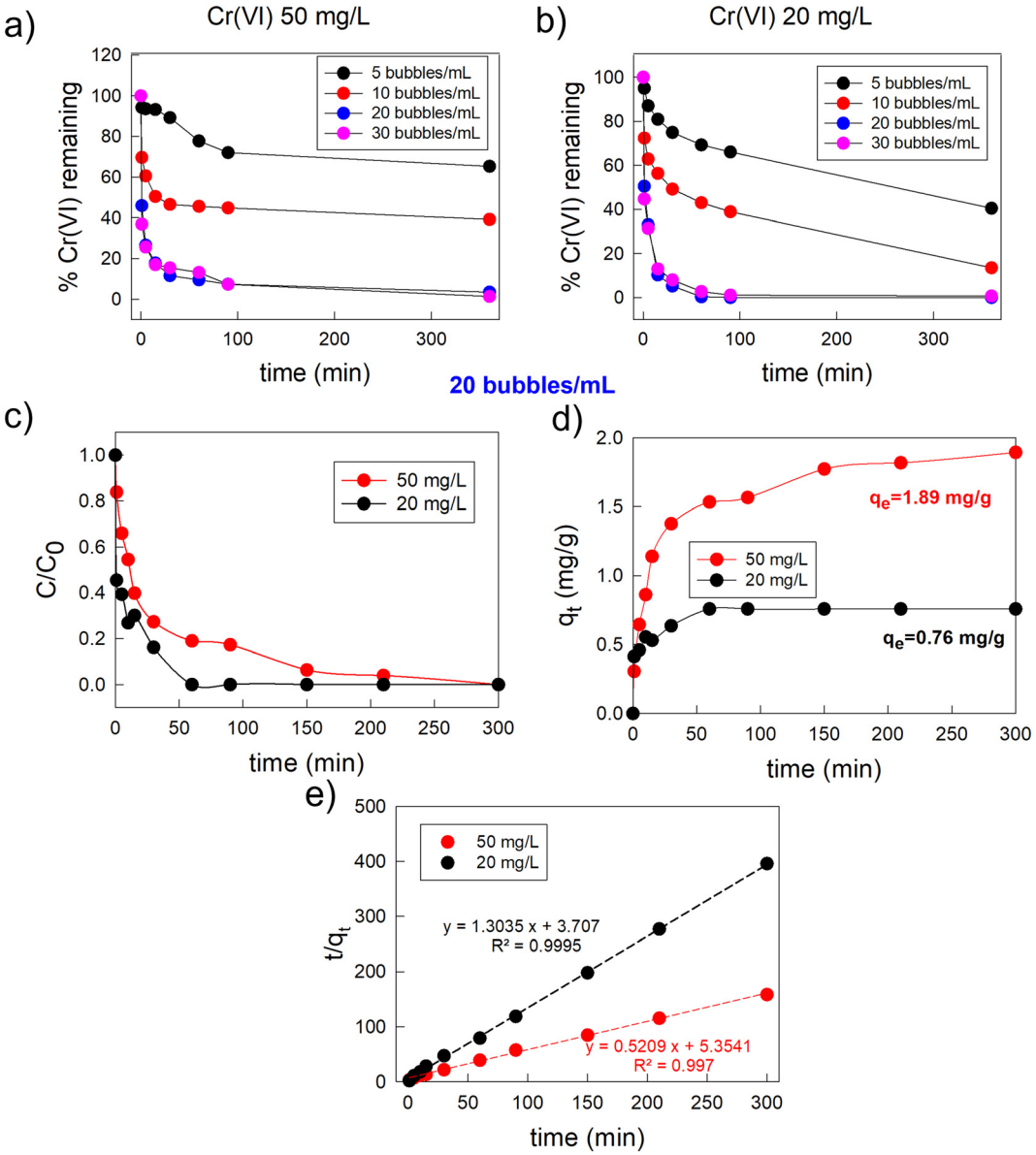

Fig. 3 (a) Lowering of the Cr(VI) concentration over time after the interaction with a variable number of Fe_3O_4/AC/VitC-alginate bubbles. Starting Cr(VI) concentration = 50 mg L^{-1} in ultrapure water. (b) Lowering of the Cr(VI) concentration over time after the interaction with a variable number of Fe_3O_4/AC/VitC-alginate bubbles. Starting Cr(VI) concentration = 20 mg L^{-1} in ultrapure water. (c) Variation of the absorbance value of the Cr(VI) solutions prepared with ultrapure water as a function of Fe_3O_4/AC/VitC-alginate bubbles' soaking time. Adsorbent dosage= 20 bubbles per mL of Cr(VI) solution. (d) Adsorption capacity of the composite Fe_3O_4/AC/VitC-alginate bubbles. (e) Pseudo-second-order adsorption isotherms of Fe_3O_4/AC/VitC-alginate bubbles. Error bars included in the point size.

bubbles per mL, 20 bubbles per mL and 30 bubbles per mL. In Fig. 3a it is possible to observe the percentage of Cr(VI) that remained in the Cr(VI) solution at different times (0–360 min) after the contact with different adsorbent loadings in the case of the MCr solution. Notably, it is possible to recognize that 20 Fe_3O_4/AC/VitC-alginate bubbles per mL of solution was the optimal loading. In fact, using a lower amount of bubbles did not enable reaching a complete Cr(VI) removal with the considered period of time. In the case of 5 Fe_3O_4/AC/VitC-alginate bubbles per mL of Cr(VI) solution, removal was limited to ~60%, while it was limited to ~85% in the case of 10 bubbles per mL. Interestingly, increasing the adsorbent loading up to 30 bubbles per mL did not enable increasing significantly the kinetics of the adsorption process, resulting only in a spoilage of adsorbent material. A similar behaviour was observed in the case of the treatment of the LCr solution, as illustrated in Fig. 3b. As a consequence, all the following experiments were conducted considering as adsorbent loading the optimal value of 20 bubbles per mL of Cr(VI) solution.

In this condition, in the case of the LCr samples, bleaching of the solution colour occurred within a few minutes (about 15 min) and complete removal of Cr(VI) was obtained after 60 min, while in the case of the MCr, complete Cr(VI) removal was obtained within 360 min, as seen in Fig. 3c, which reports the variation of the absorbance of the Cr(VI) solutions as a function of bubbles' soaking time.

As shown in tables reported in S9,† these values of adsorption time are in line or even lower than those reported in the literature for other magnetic hydrogel systems. Furthermore, it is important to highlight that our experimental protocol was intentionally designed to avoid any further post- optimization processes, such as pH modification, heating, or mixing, which could negatively impact the application of this remediation strategy. Moreover, the fact that it was possible to achieve a complete (100%) Cr(VI) removal in a short time, using low cost materials and with a very simple operation with minimal external operator intervention represents a major asset of this approach. Considering the amount of adsorbent suspended in the wastewater (~130 mg, dried weight), it was possible to calculate its adsorption capability as a function of time, which is reported in Fig. 3d. At the equilibrium time, the experimental adsorption capacity was equal to 0.76 mg g^{-1} in the case of the 20 mg L^{-1} Cr(VI) solution, which was reached after 60 min, and 1.89 mg g^{-1} in the case of the 50 mg L^{-1} Cr(VI) solution, which was reached after 360 min.

In general, it is normal to observe a rapid reduction of pollutant concentration in wastewater during the initial period of contact with the adsorbent. This functioning is linked to the availability of a large number of adsorption sites on the surface of the adsorbent at the early stage of the adsorption process, which are gradually occupied by the pollutant molecules derived from the solution and saturated over time.[60] This behaviour was observed also in the case of our composite system: in the first minute about 50% of the adsorption process occurred for the LCr sample, and a lowering of 64% of the initial absorbance value was obtained in the case of the MCr solution. After that, the adsorption rate began to slow down. This fact is particularly evident in the case of the MCr solution: in order to pass from a Cr(VI) removal of 85% (value obtained in the first 10 min) to a complete removal, it was necessary to wait for another 350 min.

In both the concentration ranges, the adsorption kinetics was represented by a pseudo-second-order model (Fig. 3e), which assumed that the rate-limiting step of the adsorption process was chemical sorption (further details about the individuation of the best kinetic model for the fitting of the adsorption data are shown in Fig. S4†). From the fitting of the experimental data, it was possible to calculate both the rate constant of the pseudo-second-order adsorption process (k_2), which was equal to 1.022 g mg^{-1} min^{-1} in the case of $[Cr^{6+}]$ = 20 mg L^{-1} and 0.2 g mg^{-1} min^{-1} for $[Cr^{6+}]$ = 50 mg L^{-1}, and the theoretical value of the equilibrium adsorption capacity, which was equal to 0.76 for $[Cr^{6+}]$ = 20 mg L^{-1} and 1.89 for $[Cr^{6+}]$ = 50 mg L^{-1}, showing a good agreement with the experimental data.

To investigate the role of each individual component of the Fe_3O_4/AC/VitC alginate bubbles, we compared their specific absorption capability with those of other alginate-based adsorbents (the considered reference systems are those listed in Table 1, and they were employed at the same dosage of ~0.132 g per 5 mL). For comparison, the contact time was fixed at 60 min. The obtained results are shown in Fig. 4a.

Among the different alginate-based bubbles, only the Fe_3O_4/AC/VitC-alginate and Fe_3O_4/VitC-alginate systems were able to guarantee a complete Cr(VI) removal in 60 minutes in the case of a Cr(VI) concentration equal to 20 mg L^{-1}. Interestingly, the system made of pure alginate was able to adsorb only 37.2% Cr(VI), while the adsorption capability was increased up to 58% after the combination of alginate with Fe_3O_4, showing that magnetite not only conferred magnetic responsiveness to the system but also slightly increased its removal capability.[61] A similar Cr(VI) removal was observed also in the case of Fe_3O_4 NPs in the form of free powder. As shown in Fig. S10,† this powder alone was able to remove ~15% Cr(VI) from the solution. In addition to physical adsorption, some chemical interactions can occur between the powder and Cr(VI): magnetite has a cubic inverse spinel structure that consists of Fe(II) and Fe(III) ions, and during the adsorbent soaking, Fe(II) can be oxidized by Cr(VI), resulting in the reduction of Cr(VI) to Cr(III).[62,63]

Coming back to hydrogel bubbles, a further adsorption enhancement, up to about 93%, was observed after the combination of alginate and Fe_3O_4 with activated carbon, probably due to the contribution of the high number of adsorption sites typical of high surface activated carbon. Complete adsorption (the remaining Cr(VI) was under the detection limit of both direct and indirect UV-vis measurements) was achieved after the addition of vitamin C (complete system: Fe_3O_4 + AC + VitC + alginate), indicating that ascorbic acid was a fundamental component for the creation of adsorbents that were characterized by high

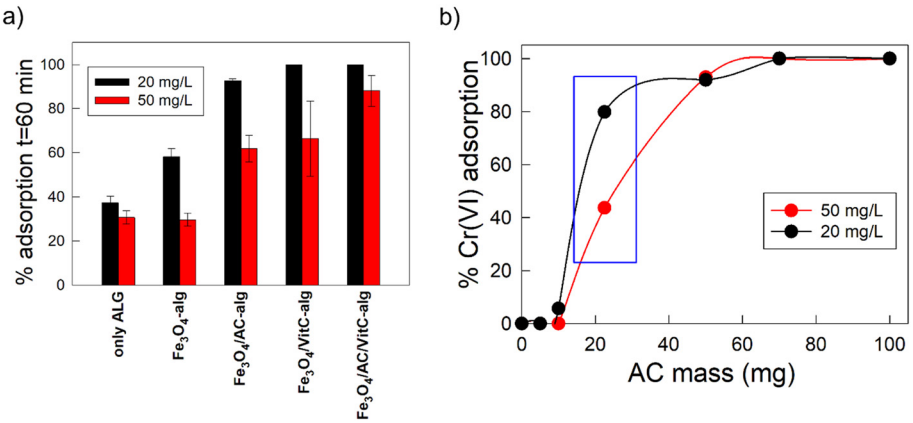

Fig. 4 (a) Percentage of Cr^{6+} removal after 60 min of contact with Fe_3O_4/VitC/AC alginate bubbles and other alginate-based adsorbent reference systems. Black data related to $[Cr^{6+}]$ = 20 mg L^{-1}, red data related to $[Cr^{6+}]$ = 50 mg L^{-1}. (b) % of Cr(VI) adsorption as a function of the increasing amount of AC in the form of free powder. Error bars are included in the point size.

removal capability. As already reported, ascorbic acid can be a key ingredient against Cr(VI), since it is able to induce its reduction to Cr(III) and obtain Cr in a more biocompatible and environmentally safe form.[19] In addition, some recent studies showed that the –COOH groups of ascorbic acid are able to complex Cr(III) and lower its dispersion in the surrounding environment.[42]

Complete removal was obtained also in the absence of activated carbon (Fe_3O_4 + Vit C + alginate bubbles). However, as reported in Fig. 4a (red bars), in the case of wastewater with a higher concentration of Cr(VI) (50 mg L^{-1}), the addition of activated carbon significantly improved the adsorption capability. The system composed of alginate, Fe_3O_4 and vitamin C after 60 minutes removed only 66.5% of Cr(VI), while for the system containing also activated carbon the removal was increased up to 88.1%. In fact, as previously reported in Fig. 3, this adsorbent could completely remove Cr(VI) at this concentration range in 360 minutes.

Activated carbon is often considered as the standard adsorbent for industrial application, since it is characterized by a huge number of adsorption sites, thanks to its high porosity and surface area. For this reason, we decided to study its adsorption capacity in the form of free powder when used under the same conditions as that of the Fe_3O_4/AC/VitC-alginate bubbles. In particular, in Fig. 4b, the variation of Cr(VI) adsorption percentage as a function of the amount of AC powder in contact for 60 minutes with 5 mL of Cr(VI) solution is reported, in the case of both Cr(VI) concentrations equal to 20 mg L^{-1} (black line) and 50 mg L^{-1} (red line). A very small amount of AC powder (*i.e.* 5 mg for $[Cr^{6+}]$ = 20 mg L^{-1} and 5 or 10 mg for $[Cr^{6+}]$ = 50 mg L^{-1}) did not enable us to obtain any Cr(VI) abatement, while complete Cr(VI) removal was obtained in both the concentration ranges when the AC powder quantity was increased up to 70 mg. However, the most relevant fact was that when the same amount of AC contained in the composite bubbles (*i.e.* 22.5 mg) was used in the form of free powder, a significant decrease of Cr(VI) removal capability was recorded. In fact, in the case of the LCr solution, Cr(VI) adsorption passes from 100% (bubbles) to ~80% (free powder), and from 86% to ~43% in the case of MCr solution. Passing from AC embedded in composite bubbles to AC in the form of free powder, a lowering of the decontamination performances was recorded for both the Cr(VI) concentration ranges, which is equal to −20% for the 20 mg L^{-1} solution and −50% for the 50 mg L^{-1} solution. These data additionally confirmed the importance of the compresence of all the building blocks in the composite system in order to guarantee a cooperation that enables maximization of the Cr(VI) removal. In fact, AC in the form of free powder would require a 3 times higher amount of pure activated carbon to achieve the same efficiency of the composite Fe_3O_4/AC/VitC alginate bubbles, with a significant increase of costs and environmental impact. Furthermore, by using adsorbent systems in the form of powder, the advantages of compactness and magnetic responsiveness related to the presence of the alginate matrix and Fe_3O_4 were lost and the full recovery was severely hampered, with possible losses of both material and adsorbed pollutant.

Finally, we verify the possibility of using the composite Fe_3O_4/AC/VitC hydrogel bubbles for Cr(VI) removal in real wastewater, that is, in the presence of other chemical inorganic species present in mineral water (see chemical analysis reported in ESI S2†) and can compete during the adsorption process. The adsorption isotherms from 1 to 420 min were collected in the case of the two different Cr(VI) concentrations (Fig. 5). The overall adsorption trends were similar to those obtained in the case of Cr(VI) solution in ultrapure water, showing a fast lowering of Cr(VI) in solution during the first minutes and a gradual decrease of the adsorption rate over time. However, in the presence of additional inorganic species, the adsorption capacity was slightly decreased. In the case of low Cr(VI) concentration, complete Cr(VI) was obtained only after 300 min. Nevertheless, it should be underlined that in the first 60 min (long enough period to achieve complete removal in ultrapure water) Cr(VI) removal was as high as 93%. In the

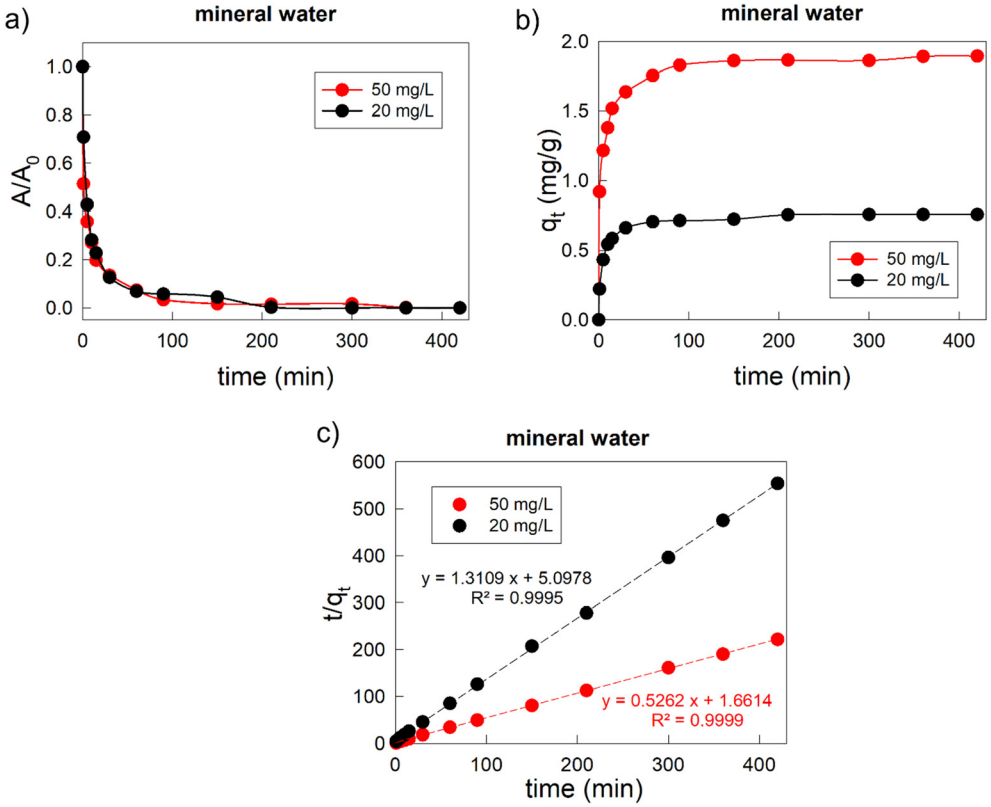

Fig. 5 (a) Variation of the absorbance value of the Cr(VI) solutions prepared with mineral water as a function of Fe_3O_4/AC/VitC-alginate bubbles' soaking time. (b) Adsorption capacity of the composite Fe_3O_4/AC/VitC-alginate bubbles against Cr(VI) wastewater in the presence of common competitive chemical species. Error bars included in the point size. c) Pseudo-second-order adsorption isotherms in mineral water. Error bars are included in the point size.

case of the medium concentration range, complete Cr(VI) was obtained in 420 min, but also in this case 93% of Cr(VI) was adsorbed in the first 60 min. As shown in Fig. 5c, also in real water the adsorption process occurred through pseudo-second-order kinetics.

The decrease of the percentage of adsorbed Cr(VI) and the increase of time needed to achieve complete Cr(VI) removal were due to the competition during the adsorption process of other ions contained in real wastewater, which were characterized by a significantly higher concentration than that of Cr(VI), as reported in ESI S2.† In particular, bicarbonate (232 mg L^{-1}) could affect Cr(VI) adsorption in different ways: on one hand, it has the same negative charge as bichromate or chromate (the chemical species from which Cr(VI) derives) and could compete for positively charged adsorption sites; on the other hand, it could contribute in raising the pH value. In fact, when Cr(VI) solutions were prepared in ultrapure water they were characterised by a pH of 6.34 for the 20 mg L^{-1} concentration and 5.5 for the 50 mg L^{-1} sample, while solutions obtained in mineral water were characterized by a less acidic pH (7.9 for the 20 mg L^{-1} concentration and 7.7 for the 50 mg L^{-1} sample). This variation of pH could modify the surface charge of the adsorbent and the chemical form in which Cr is present in the solution ($HCrO_4^-$ is the predominant species at pH <6.5, while CrO_4^{2-} is the main Cr(VI) form for pH above 6.5). In addition, bicarbonate could induce a rapid decomposition of vitamin C, lowering the effectiveness of its reductive interaction with Cr(VI).[64] All these facts could hinder the adsorption process of the Fe_3O_4/AC/VitC hydrogel bubbles. The lowering of adsorption performance and the slowing down of the adsorption process were more significant in the case of low Cr(VI) concentration; in fact, the kinetic constant passed from 1.022 g mg^{-1} min^{-1} (in ultrapure water) to 0.34 g mg^{-1} min^{-1} (in mineral water). In the higher concentration case, instead, the variation of the kinetic constant was minor: it passed from 0.20 g mg^{-1} min^{-1} to 0.17 g mg^{-1} min^{-1}.

4. Conclusions

Magnetic hydrogels composed of magnetite, activated carbon, and L-ascorbic acid in calcium-cross-linked alginate bubbles showed an efficient and fast removal of Cr(VI) in the concentration range 20–50 mg L^{-1}. Even if this range is well above the discharge limit in wastewaters for European countries (*i.e.* Italy: 2–4 mg L^{-1} for total Cr and 0.2 mg L^{-1} Cr(VI)) or many Asian countries (*i.e.* Thailand: 0.25 mg L^{-1} and 0.75 mg L^{-1} for Cr(VI) and Cr(III), respectively), this investigation is of great environmental relevance. In fact, in many Asian countries the actual Cr concentrations in discharged industrial wastewater range usually from 10 to almost 100 mg L^{-1} (ref. 65–67) and the here-proposed

Fe_3O_4/AC/VitC-alginate bubbles could provide fast and efficient remediation under these conditions. The high removal capability of these systems was the result of the synergistic interplay between the single components: the alginate matrix and activated carbon conferred to the system high adsorption capacity, while ascorbic acid enabled combining a redox and a chelating activity. The outcome was that, in comparison to the plain alginate counterpart or other alginate-based hydrogels containing only some of the aforementioned components, the complete composite system was characterized by a significantly improved decontaminant activity. Interestingly, it was also capable of outperforming commercial activated carbon employed in the form of free powder.

Additionally, thanks to the presence of magnetite, the proposed adsorbent could be easily collected after the completion of the decontamination activity through the application of external magnetic fields, with a high potential of subsequent purification and regeneration processes.

With the promising results shown in relation to ultrapure water, we investigated the activity in the case of Cr(VI)-contaminated mineral water. Even if a slowing down of the removal process was observed, probably because of the competition during the adsorption process of other ions contained in the solution, the composite bubbles were still able to completely abate Cr(VI) in limited periods (maximum 420 minutes).

The advantages related to the use of the Fe_3O_4/AC/VitC alginate hydrogel bubbles are not limited to only high adsorption capability but also to high environmental sustainability and low cost. The hydrogels were synthesised in one step from affordable nature-based materials, like ascorbic acid and sodium alginate, combined with magnetite particles obtained from mill scale, which is consistently generated as industrial waste in a large amount every year. In this perspective, the fabrication of Fe_3O_4/AC/VitC hydrogel bubbles is a win-win approach, since it enables conversion of an industrial waste into a high value-added product and resolution of an environmental problem, such as high concentrations of Cr(VI) in water. Furthermore, all the expenses normally sustained for the disposal of this industrial waste can be avoided. From the economic point of view, the proposed adsorbent is characterized by a low impact: alginate is relatively cheap[68] and, eventually, it can be extracted in the laboratory from brown algae seaweeds; similar considerations can be done for ascorbic acid, which can be extracted from various vegetables scraps. Activated carbon is the most expensive component, but after encapsulation inside the bubble structure a smaller amount (in comparison to free powder) is enough to obtain complete Cr(VI) removal, limiting the increase of adsorbent cost. In addition, the fabrication process of the hydrogel composite system as well as the Cr(VI) adsorption process is very simple and suitable for industrial and commercial-scale development. In terms of sustainability, the hydrogel bubbles could be further improved by replacing commercial activated carbon, since its production relies on fossil fuels, with other recycling materials, leaving space for further development of the here-proposed system. Moreover, additional properties, such as recyclability and photo-degradation activity, could be investigated and optimized in order to ensure a complete eco-friendly behaviour of the Fe_3O_4/AC/VitC-alginate hydrogel bubbles.

Conflicts of interest

There are no conflicts to declare.

Acknowledgements

The research is funded by a Research and Researchers for Industries scholarship under Thailand Research Fund (Contract number PHD60I0081). I. V. is partially supported by the Italian Ministry of University and Research (MUR) through the PRIN project NOMEN (2017MP7F8F).

References

1 A. di Schino, in *Handbook of Environmental Materials Management*, Springer, Cham, 2017, pp. 1–21.
2 C. Broadbent, Steel's recyclability: demonstrating the benefits of recycling steel to achieve a circular economy, *Int. J. Life Cycle Assess.*, 2016, **21**, 1658–1665.
3 D.-A. Iluțiu-Varvara, C. Aciu, M. Tintelecan and I.-M. Sas-Boca, Assessment of Recycling Potential of the Steel Mill Scale in the Composition of Mortars for Sustainable Manufacturing, *Procedia Manuf.*, 2020, **46**, 131–135.
4 K. Nowacki, T. Maciąg and T. Lis, Recovery of Iron from Mill Scale by Reduction with Carbon Monoxide, *Minerals*, 2021, **11**, 529.
5 R. Rakhunde, L. Deshpande and H. D. Juneja, Chemical Speciation of Chromium in Water: A Review, *Crit. Rev. Environ. Sci. Technol.*, 2012, **42**, 776–810.
6 M. Maddaloni, I. Alessandri and I. Vassalini, Food-waste enables carboxylated gold nanoparticles to completely abate hexavalent chromium in drinking water, *Environ. Nanotechnol., Monit. Manage.*, 2022, **18**, 100686.
7 N. A. A. Qasem, R. H. Mohammed and D. U. Lawal, Removal of heavy metal ions from wastewater: a comprehensive and critical review, *npj Clean Water*, 2021, **4**, 1–15.
8 Z. Li, X. Zhang and L. Lei, Electricity production during the treatment of real electroplating wastewater containing Cr^{6+} using microbial fuel cell, *Process Biochem.*, 2008, **43**, 1352–1358.
9 T. M. Zewail and N. S. Yousef, Chromium ions (Cr^{6+} & Cr^{3+}) removal from synthetic wastewater by electrocoagulation using vertical expanded Fe anode, *J. Electroanal. Chem.*, 2014, **735**, 123–128.
10 G. Basaran, D. Kavak, N. Dizge, Y. Asci, M. Solener and B. Ozbey, Comparative study of the removal of Nickel(II) and Chromium(VI) heavy metals from metal plating wastewater by two nanofiltration membranes, *Desalin. Water Treat.*, 2016, **57**, 21870–21880.

11 L. I. Mengqi, Y. Chunfeng, Z. Kai, S. U. N. Jingqiu, L. I. Jing, L. U. O. Lining and H. U. Chengzhi, Removal of Cr(VI) from wastewater by electrocoagulation membrane reactor based on reduction, flocculation and ultrafiltration, *Huanjing Gongcheng Xuebao*, 2018, **12**, 79–85.
12 S. De Gisi, G. Lofrano, M. Grassi and M. Notarnicola, Characteristics and adsorption capacities of low-cost sorbents for wastewater treatment: A review, *Sustainable Mater. Technol.*, 2016, **9**, 10–40.
13 V. E. Pakade, N. T. Tavengwa and L. M. Madikizela, Recent advances in hexavalent chromium removal from aqueous solutions by adsorptive methods, *RSC Adv.*, 2019, **9**, 26142–26164.
14 G. Crini, E. Lichtfouse, L. D. Wilson and N. Morin-Crini, in *Green Adsorbents for Pollutant Removal: Fundamentals and Design*, ed. G. Crini and E. Lichtfouse, Springer International Publishing, Cham, 2018, pp. 23–71.
15 G. Crini, E. Lichtfouse, L. D. Wilson and N. Morin-Crini, Conventional and non-conventional adsorbents for wastewater treatment, *Environ. Chem. Lett.*, 2019, **17**, 195–213.
16 T. A. Aragaw and F. M. Bogale, Biomass-Based Adsorbents for Removal of Dyes from Wastewater: A Review, *Front. Environ. Sci.*, 2021, **9**, 764958.
17 D. A. Gkika, A. C. Mitropoulos and G. Z. Kyzas, Why reuse spent adsorbents? The latest challenges and limitations, *Sci. Total Environ.*, 2022, **822**, 153612.
18 D. Chen, L. Wang, Y. Ma and W. Yang, Super-adsorbent material based on functional polymer particles with a multilevel porous structure, *NPG Asia Mater.*, 2016, **8**, e301.
19 I. Vassalini, M. Litvinava and I. Alessandri, All food waste-based membranes for Chromium(VI) removal, *Environ. Sustainability*, 2020, **4**, 1–7.
20 A. Jeyaseelan, I. A. Kumar, M. Naushad and N. Viswanathan, Defluoridation using hydroxyapatite implanted lanthanum organic framework-based bio-hybrid beads, *React. Chem. Eng.*, 2022, **7**, 2107–2120.
21 A. Jeyaseelan, I. A. Kumar, N. Viswanathan and M. Naushad, Development and characterization of hydroxyapatite layered lanthanum organic frameworks by template method for defluoridation of water, *J. Colloid Interface Sci.*, 2022, **622**, 228–238.
22 A. Jeyaseelan, I. A. Kumar, M. Naushad and N. Viswanathan, Enhanced and fast fluoride adsorption using cerium organic frameworks based hydrotalcite hybrid material, *J. Rare Earths*, 2023, **41**, 2010–2017.
23 I. Vassalini, G. Ribaudo, A. Gianoncelli, M. F. Casula and I. Alessandri, Plasmonic hydrogels for capture, detection and removal of organic pollutants, *Environ. Sci.: Nano*, 2020, **7**, 3888–3900.
24 I. Vassalini, N. Bontempi, S. Federici, M. Ferroni, A. Gianoncelli and I. Alessandri, Cyclodextrins enable indirect ultrasensitive Raman detection of polychlorinated biphenyls captured by plasmonic bubbles, *Chem. Phys. Lett.*, 2021, **775**, 138674.
25 H. K. Agbovi and L. Wilson, in *Adsorption processes in biopolymer systems: fundamentals to practical applications*, 2021, pp. 1–51.
26 L. A. Shah and S. A. Khan, in *Environmental Chemistry and Recent Pollution Control Approaches*, ed. H. Saldarriaga-Norena, M. A. Murillo-Tovar, R. Farooq, R. Dongre and S. Riaz, IntechOpen, 2019.
27 D. M. Roquero and E. Katz, "Smart" alginate hydrogels in biosensing, bioactuation and biocomputing: State-of-the-art and perspectives, *Sens. Actuators Rep.*, 2022, **4**, 100095.
28 A. G. Corpuz, P. Pal, F. Banat and M. A. Haija, Enhanced removal of mixed metal ions from aqueous solutions using flotation by colloidal gas aphrons stabilized with sodium alginate, *Sep. Purif. Technol.*, 2018, **202**, 103–110.
29 N. Yang, R. Wang, P. Rao, L. Yan, W. Zhang, J. Wang and F. Chai, The Fabrication of Calcium Alginate Beads as a Green Sorbent for Selective Recovery of Cu(II) from Metal Mixtures, *Crystals*, 2019, **9**, 255.
30 J. Shim, M. Kumar, S. Mukherjee and R. Goswami, Sustainable removal of pernicious arsenic and cadmium by a novel composite of MnO_2 impregnated alginate beads: A cost-effective approach for wastewater treatment, *J. Environ. Manage.*, 2019, **234**, 8–20.
31 A. Sigdel, J. Lim, J. Park, H. Kwak, S. Min, K. Kim, H. Lee, C. H. Nahm and P.-K. Park, Immobilization of hydrous iron oxides in porous alginate beads for arsenic removal from water, *Environ. Sci.: Water Res. Technol.*, 2018, **4**, 1114–1123.
32 Y. Mo, S. Wang, T. Vincent, J. Desbrieres, C. Faur and E. Guibal, New highly-percolating alginate-PEI membranes for efficient recovery of chromium from aqueous solutions, *Carbohydr. Polym.*, 2019, **225**, 115177.
33 Y. He, J. Chen, J. Lv, Y. Huang, S. Zhou, W. Li, Y. Li, F. Chang, H. Zhang, T. Wågberg and G. Hu, Separable amino-functionalized biochar/alginate beads for efficient removal of Cr(VI) from original electroplating wastewater at room temperature, *J. Cleaner Prod.*, 2022, **373**, 133790.
34 V. Gopalakannan and N. Viswanathan, Synthesis of magnetic alginate hybrid beads for efficient chromium (VI) removal, *Int. J. Biol. Macromol.*, 2015, **72**, 862–867.
35 R. Wen, B. Tu, X. Guo, X. Hao, X. Wu and H. Tao, An ion release controlled Cr(VI) treatment agent: Nano zero-valent iron/carbon/alginate composite gel, *Int. J. Biol. Macromol.*, 2020, **146**, 692–704.
36 W. Liang, Y. Shen, C. Xu, D. Cai, D. Wang, K. Luo, X. Shao, Z. Qiao, W. Zhang and C. Peng, Enhanced simultaneous removal of Cr(VI) and Cd(II) from aqueous solution and soil: a novel carbon microsphere–calcium alginate supported sulfide-modified nZVI composite, *Environ. Sci.: Nano*, 2022, **9**, 3471–3484.
37 P. A. Augusto, T. Castelo-Grande, D. Vargas, A. Pascual, L. Hernández, A. M. Estevez and D. Barbosa, Upscale Design, Process Development, and Economic Analysis of Industrial Plants for Nanomagnetic Particle Production for Environmental and Biomedical Use, *Materials*, 2020, **13**, 2477.
38 Y. E. Gunanto, M. P. Izaak, E. Jobiliong, L. Cahyadi and W. A. Adi, High purity Fe_3O_4 from Local Iron Sand Extraction, *J. Phys.: Conf. Ser.*, 2018, **1011**, 012005.
39 A. Boontanom and P. Suwanpinij, in *Materials Science Forum*, ed. M. Ionescu, C. Sommitsch, C. Poletti, E. Kozeschnik and

T. Chandra, Trans Tech Publications, Switzerland, 2020, vol. 1016, pp. 288–291.

40 H. Chun and Y. Choi, A Study on the Mill Scale Pretreatment and Magnetite Production for Phosphate Adsorption, *J. Korean Soc. Environ. Eng.*, 2015, **37**, 246–252.

41 H. A. Al-Abadleh, A. L. Mifflin, M. J. Musorrafiti and F. M. Geiger, Kinetic Studies of Chromium (VI) Binding to Carboxylic Acid- and Methyl Ester-Functionalized Silica/Water Interfaces Important in Geochemistry, *J. Phys. Chem. B*, 2005, **109**, 16852–16859.

42 X.-R. Xu, H.-B. Li, X.-Y. Li and J.-D. Gu, Reduction of hexavalent chromium by ascorbic acid in aqueous solutions, *Chemosphere*, 2004, **57**, 609–613.

43 X. Wu, Y. Xu, Y. Dong, X. Jiang and N. Zhu, Colorimetric determination of hexavalent chromium with ascorbic acid capped silver nanoparticles, *Anal. Methods*, 2012, **5**, 560–565.

44 H.-Y. Lin, Y.-W. Chen and C. Li, The mechanism of reduction of iron oxide by hydrogen, *Thermochim. Acta*, 2003, **400**, 61–67.

45 W. K. Jozwiak, E. Kaczmarek, T. P. Maniecki, W. Ignaczak and W. Maniukiewicz, Reduction behavior of iron oxides in hydrogen and carbon monoxide atmospheres, *Appl., Catal. A*, 2007, **326**, 17–27.

46 A. Sanchez-Hachair and A. Hofmann, Hexavalent chromium quantification in solution: Comparing direct UV–visible spectrometry with 1,5-diphenylcarbazide colorimetry, *C. R. Chim.*, 2018, **21**, 890–896.

47 G. Vijayakumar, R. Tamilarasan and M. Dharmendirakumar, Adsorption, Kinetic, Equilibrium and Thermodynamic studies on the removal of basic dye Rhodamine-B from aqueous solution by the use of natural adsorbent perlite, *J. Mater. Environ. Sci.*, 2012, **3**, 157–170.

48 O. N. Shebanova and P. Lazor, Raman spectroscopic study of magnetite ($FeFe_2O_4$): a new assignment for the vibrational spectrum, *J. Solid State Chem.*, 2003, **174**, 424–430.

49 N. A. A. Nazri, R. S. Azis, H. C. Man, I. Ismail and I. R. Ibrahim, Extraction of Magnetite from Millscales Waste for Ultrafast Removal of Cadmium Ions, *Int. J. Eng. Adv. Technol.*, 2019, **9**, 5902–5907.

50 A. G. Kolhatkar, A. C. Jamison, D. Litvinov, R. C. Willson and T. R. Lee, Tuning the Magnetic Properties of Nanoparticles, *Int. J. Mol. Sci.*, 2013, **14**, 15977–16009.

51 V. Phouthavong, R. Yan, S. Nijpanich, T. Hagio, R. Ichino, L. Kong and L. Li, Magnetic Adsorbents for Wastewater Treatment: Advancements in Their Synthesis Methods, *Materials*, 2022, **15**, 1053.

52 E. D. Smolensky, H.-Y. E. Park, Y. Zhou, G. A. Rolla, M. Marjańska, M. Botta and V. C. Pierre, Scaling laws at the nanosize: the effect of particle size and shape on the magnetism and relaxivity of iron oxide nanoparticle contrast agents, *J. Mater. Chem. B*, 2013, **1**, 2818–2828.

53 A. M. Huízar-Félix, C. Aguilar-Flores, A. Martínez-de-la Cruz, J. M. Barandiarán, S. Sepúlveda-Guzmán and R. Cruz-Silva, Removal of Tetracycline Pollutants by Adsorption and Magnetic Separation Using Reduced Graphene Oxide Decorated with α-Fe2O3 Nanoparticles, *Nanomaterials*, 2019, **9**, 313.

54 S. C. N. Tang, D. Y. S. Yan and I. M. C. Lo, Sustainable Wastewater Treatment Using Microsized Magnetic Hydrogel with Magnetic Separation Technology, *Ind. Eng. Chem. Res.*, 2014, **53**, 15718–15724.

55 Y. Liu, J. S. Wang, P. Zhy, J. C. Zhao, C. J. Zhang, Y. Gao and L. Cui, Thermal degradation properties of biobased iron alginate film, *J. Anal. Appl. Pyrolysis*, 2016, **119**, 87–96.

56 N. Rescignano, R. Hernandez, L. D. Lopez, I. Calvillo, J. M. Kenny and C. Mijangos, Preparation of alginate hydrogels containing silver nanoparticles: a facile approach for antibacterial applications, *Polym. Int.*, 2016, **65**, 921–926.

57 B. Kusuktham, J. Prasertgul and P. Srinun, Morphology and Property of Calcium Silicate Encapsulated with Alginate Beads, *Silicon*, 2014, **6**, 191–197.

58 S. Mura, Y. Jiang, I. Vassalini, A. Gianoncelli, I. Alessandri, G. Granozzi, L. Calvillo, N. Senes, S. Enzo, P. Innocenzi and L. Malfatti, Graphene Oxide/Iron Oxide Nanocomposites for Water Remediation, *ACS Appl. Nano Mater.*, 2018, **1**, 6724–6732.

59 I. Vassalini, J. Gjipalaj, S. Crespi, A. Gianoncelli, M. Mella, M. Ferroni and I. Alessandri, Alginate-Derived Active Blend Enhances Adsorption and Photocatalytic Removal of Organic Pollutants in Water, *Adv. Sustainable Syst.*, 2020, **4**, 1900112.

60 S. Xie, Z. Wen, H. Zhan and M. Jin, An Experimental Study on the Adsorption and Desorption of Cu(II) in Silty Clay, *Geofluids*, 2018, **2018**, e3610921.

61 C. Kim, S. S. Lee, B. J. Lafferty, D. E. Giammar and J. D. Fortner, Engineered superparamagnetic nanomaterials for arsenic(V) and chromium(VI) sorption and separation: quantifying the role of organic surface coatings, *Environ. Sci.: Nano*, 2018, **5**, 556–563.

62 K. Simeonidis, E. Kaprara, T. Samaras, M. Angelakeris, N. Pliatsikas, G. Vourlias, M. Mitrakas and N. Andritsos, Optimizing magnetic nanoparticles for drinking water technology: The case of Cr(VI), *Sci. Total Environ.*, 2015, **535**, 61–68.

63 D. Mahringer, C. Polenz and F. El-Athman, Stabilization of Chromium (VI) in the Presence of Iron (II): Method Development and Validation, *Water*, 2020, **12**, 924.

64 P. J. Jansson, H. R. Jung, C. Lindqvist and T. Nordström, Oxidative Decomposition of Vitamin C in Drinking Water, *Free Radical Res.*, 2004, **38**, 855–860.

65 W. Liu and Y. Yu, Ultrafast advanced treatment of chromium complex-containing wastewater using Co/Fe layered double hydroxide, *Environ. Technol. Innovation*, 2022, **26**, 102296.

66 G. Moussavi, F. Jiani and S. Shekoohiyan, Advanced reduction of Cr(VI) in real chrome-plating wastewater using a VUV photoreactor: Batch and continuous-flow experiments, *Sep. Purif. Technol.*, 2015, **151**, 218–224.

67 S. Sangkarak, A. Phetrak, S. Kittipongvises, D. Kitkaew, D. Phihusut and J. Lohwacharin, Adsorptive performance of activated carbon reused from household drinking water filter for hexavalent chromium-contaminated water, *J. Environ. Manage.*, 2020, **272**, 111085.

68 L. Marchi, F. Dinelli, P. Maccagnani, V. Costa, T. Chenet, G. Belleti, M. Natali, M. Cocchi, M. Bertoldo and M. Seri, Sodium Alginate as a Natural Substrate for Efficient and Sustainable Organic Solar Cells, *ACS Sustainable Chem. Eng.*, 2022, **10**, 15608–15617.